Journal of Asian Ceramic Societies

ISSN: (Print) (Online) Journal homepage: https://www.tandfonline.com/loi/tace20

Apatite formation on electrochemically modified surface of hafnium metal in simulated body environment

Toshiki Miyazaki & Yosuke Sudo

To cite this article: Toshiki Miyazaki & Yosuke Sudo (2022) Apatite formation on electrochemically modified surface of hafnium metal in simulated body environment, Journal of Asian Ceramic Societies, 10:1, 215-222, DOI: 10.1080/21870764.2022.2034249

To link to this article: https://doi.org/10.1080/21870764.2022.2034249

Published online: 17 Feb 2022.

JOURNAL OF ASIAN CERAMIC SOCIETIES
2022, VOL. 10, NO. 1, 215–222
https://doi.org/10.1080/21870764.2022.2034249

THE CERAMIC SOCIETY OF JAPAN
THE KOREAN CERAMIC SOCIETY
Taylor & Francis
Taylor & Francis Group

FULL LENGTH ARTICLE

Apatite formation on electrochemically modified surface of hafnium metal in simulated body environment

Toshiki Miyazaki[1,2] and Yosuke Sudo[1]

[1]Graduate School of Life Science and System Engineering, Kyushu Institute of Technology, Kitakyushu, Japan; [2]Collaborative Research Centre for Green Materials on Environmental Technology, Kyushu Institute of Technology, Kitakyushu, Japan

ABSTRACT

Biomedical application of Hf for hard tissue repair may be expanded if it can be imparted with bone-bonding ability. Apatite formation in the body is required for artificial materials to bond to bone. We have shown that apatite can form on NaOH- and heat-treated Hf in simulated body fluid, although the degree of apatite formation is not high. In this study, we investigated apatite formation on surface-modified Hf metal in simulated body fluid. Hf substrates were soaked in NH_4F solution or electrochemically polarized in H_2SO_4 or NH_4F solution, followed by heating at 600°C. The sample soaked or cathodically polarized in NH_4F solution had porous structure, and the anodically polarized sample had nanotube aggregates on its surface. F was incorporated into the sample polarized in NH_4F solution, but not the sample merely soaked in the solution. NH_4F was more effective than H_2SO_4 in facilitating apatite formation. Remarkably, the sample soaked in NH_4F solution had the highest apatite-forming ability. Its porous structure was considered to play a dominant role in apatite formation. Furthermore, there was little correlation between surface energy and apatite formation. Notably, NH_4F treatment is more effective than the previously reported NaOH and heat treatments in promoting apatite formation.

ARTICLE HISTORY
Received 2 December 2021
Accepted 22 January 2022

KEYWORDS
Hafnium; apatite formation; electrochemical polarization; ammonium fluoride; simulated body fluid

1. Introduction

Hf belongs to the same group 4 elements as Ti and Zr which are used for hard tissue repair. Therefore, Hf is expected to be biologically compatible similar to Ti and Zr. Actually, it is reported that pure Hf shows osseointegration where it morphologically integrates with bone tissue of rat femur [1]. However, even when the metals show the osseointegration, the bond strength is very low [2–4]. Low-crystalline apatite formed on the implanted surface by reaction with body fluid is required for artificial materials to bond tightly to bone [5]. Apatite can form in simulated body fluid (SBF) with inorganic ion concentrations similar to that of extracellular fluid [6–8]. For this purpose, various chemical surface modifications of the artificial material have been proposed [9,10].

Although pure Hf has not been clinically used, various alloys with high Hf content have been developed for biomedical applications. For example, it is known that tensile strength and hardness of Ti-40Hf alloy are higher than pure Ti [11]. Anodized Ti-40Hf shows enhanced corrosion resistance compared to pure Ti [12]. Also, Ti-Nb-Hf-Zr alloy with Hf content of 16 mass% has been proposed for the purpose of reducing the elasticity of Ti [13]. Therefore, improvement of bone-bonding ability of Hf is considered to be meaningful.

We have previously reported that apatite formation was observed on pure Hf and Ti-Hf alloy in SBF after NaOH and heat treatments [14], although their apatite-forming abilities were lower than those of NaOH- and heat-treated Ti. Yang *et al*. demonstrated that anodic polarization can facilitate apatite formation on Ti metal [15]. In addition, TiO_2 nanotubes can be constructed on the Ti surface via anodic polarization in a fluoride solution [16], and this specific porous structure is effective for sustained drug release [17]. Notably, anodic polarization can also be used to fabricate HfO_2 nanotubes on Hf metal [18].

In this study, we investigated the apatite-forming ability of Hf metal in SBF after the various surface modifications: different electrochemical polarizations in a solution of H_2SO_4 or NH_4F and soaking in a solution of NH_4F.

2. Materials and methods

2.1. Sample preparation

The reagents used to prepare SBF were purchased from Nacalai Tesque Inc. (Kyoto, Japan). The other reagents were purchased from FUJIFILM Wako Pure Chemical Co. (Osaka, Japan). Hf plates of 0.1x10x10 mm in size (The Nilaco Co., Tokyo, Japan) were used as the substrate. The surfaces were dry-grinded with #500 SiC water-

CONTACT Toshiki Miyazaki tmiya@life.kyutech.ac.jp Graduate School of Life Science and Systems Engineering, Kyushu Institute of Technology, 2-4, Hibikino, Wakamatsu-ku, Kitakyushu 808-0196, Japan

resistant abrasive paper. In the polarization treatment, Hf plates were used as both the anode and the cathode. The substrates were anodically polarized in 3 M H_2SO_4 at 30 V for 20 min or in a solution containing 16 mL of ethylene glycol, 4 mL of ultrapure water, and 0.1 mol of NH_4F at 30 V for 20 or 60 min. To determine the solution composition, we referred to a previous report [18].

Cathode polarization treatment was performed in the above NH_4F-containing solution step-by-step at 15 V, 30 V, and 45 V [17]. Samples were kept for 20 min at each voltage. Furthermore, Hf plates were soaked in a solution containing 20 mL of ultrapure water, 80 mL of formamide, and 0.1 mol of NH_4F at room temperature for 60 min.

The samples subjected to the above treatments were subsequently heated at 600°C for 1 h using an electric furnace (300Plus, DENKEN-HIGHDENTAL Co., Ltd., Kyoto, Japan). The samples heat-treated after anodic polarization in H_2SO_4 solution for 20 min, anodic polarization in NH_4F solution for 20 or 60 min, cathodic polarization in NH_4F solution for 20 min, and soaking in NH_4F solution for 60 min are hereafter denoted as SA, FA20, FA60, FC, and FS, respectively.

2.2. Soaking in SBF

The treated substrates were soaked in 30 mL of SBF containing 142.0 mM Na^+, 5.0 mM K^+, 2.5 mM Mg^{2+}, 147.8 mM Cl^-, 4.2 mM HCO_3^-, 1.0 mM HPO_4^{2-}, and 0.5 mM SO_4^{2-} at 36.5°C for various time periods. The pH of the solution was buffered at 7.40 using 50 mM tris(hydroxymethyl)aminomethane and an appropriate amount of HCl. The SBF was prepared in accordance with reported procedures [6–8]. After the substrates were soaked in SBF, they were removed from the SBF and then washed with ultrapure water for 30 min to remove excess water-soluble salts on their surfaces.

2.3. Characterization

The substrate surfaces were characterized using scanning electron microscopy (SEM, S-3500 N, Hitachi Co., Tokyo, Japan), field emission scanning electron microscopy (FE-SEM, JSM-7800 F, JEOL Ltd., Tokyo, Japan), energy dispersive X-ray spectroscopy (EDX, EX-400, Horiba Co., Kyoto, Japan), and thin-film X-ray diffraction (TF-XRD, MXP3V, Mac Science Ltd., Yokohama, Japan). In the TF-XRD experiments, CuKα X-ray with a voltage of 40 kV and a current of 30 mA was used. The incident beam was fixed at 1° to the surface of each substrate, and the scan rate was 0.02°·s^{-1}. All the specimens were coated with an Au-Pd thin film before SEM observations using an ion sputter (E-101, Hitachi Co., Tokyo, Japan). The atomic ratio of each element was calculated from the peak areas of the EDX spectrum.

Contact angles were measured using a contact angle meter (DMe-200, Kyowa Interface Science Co., Ltd, Saitama, Japan). The surface energy was calculated from the contact angles determined using ultrapure water and CH_2I_2. The following equations of the Owens and Wendt theory were used [19]:

$$\sqrt{\gamma_S^d \cdot \gamma_{H2O}^d} + \sqrt{\gamma_S^h \cdot \gamma_{H2O}^h} = \frac{\gamma_{H2O}(1+\cos\theta_{H2O})}{2} \quad (1)$$

$$\sqrt{\gamma_S^d \cdot \gamma_{CH2I2}^d} + \sqrt{\gamma_S^h \cdot \gamma_{CH2I2}^h} = \frac{\gamma_{CH2I2}(1+\cos\theta_{CH2I2})}{2} \quad (2)$$

$$\gamma_X = \gamma_X^d + \gamma_X^h \ (X = s, H_2O, CH_2I_2) \quad (3)$$

where γ_x ($X = H_2O, CH_2I_2$) is the total surface energy per unit area in medium X and γ_S is the total surface energy of the solid sample. Additionally, γ_x^d and γ_x^h are dispersion components based on dipole-dipole interactions and hydrogen bonding, respectively. The values of γ_{H2O}^d and γ_{H2O}^h were respectively 21.8 and 51.0 mJ·m^{-2}, and the values of γ_{CH2I2}^d and γ_{CH2I2}^h were respectively 49.5 and 1.3 mJ·m^{-2}. The contact angles θ_{H2O} and θ_{CH2I2} were measured using water and CH_2I_2, respectively.

3. Results

Table 1 shows the F content of the samples after various treatments. FA20 and FC contained approximately 0.1% F, and SA and FS did not contain any F.

Figure 1 shows FE-SEM photograph of the surface of a sample anodically polarized in NH_4F solution. The surface contained aggregates of nanotubes with a pore size of approximately 30 nm. Figure 2 shows SEM photographs of SA and FA20 before and after soaking in SBF. A rough surface was observed before soaking, and spherical particles were observed after both substrates were soaked in SBF. The degree of particle coverage was higher in FA20 than in SA. Figure 3 shows the TF-XRD patterns of the same samples. The formation of monoclinic HfO_2 (JCPDS #34-0104) was observed for both SA and FA20. After soaking in SBF, a small diffraction peak assigned to apatite (JCPDS #09-0432) was detected only in FA20. Table 2 shows the elemental composition of the apatite formed on FA20. The composition of F was 0.14%, and the Ca/P molar ratio of apatite was 1.80 higher than the stoichiometric value of hydroxyapatite (1.67).

Table 1. F content of the samples after various treatments.

Sample	F/(F + O+ Hf)
SA	0
FA20	0.179 ± 0.00721
FC	0.165 ± 0.0207
FS	0

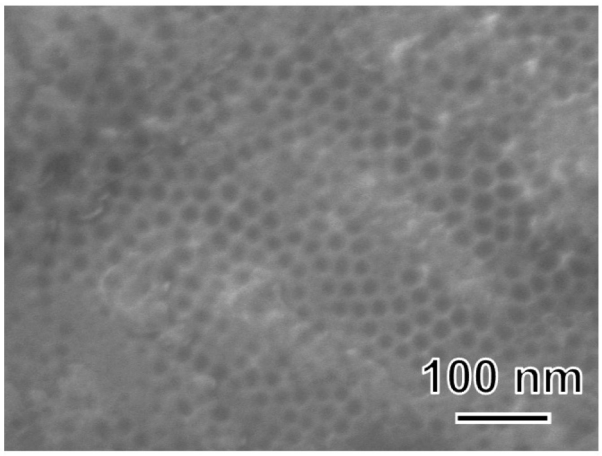

Figure 1. FE-SEM photograph of Hf substrate anodically polarized in NH_4F solution.

Figure 4 shows the TF-XRD pattern and SEM photograph of FA60 before and after soaking in SBF for 3 days. After FA60 was soaked in SBF, apatite peaks were observed and the spherical particles covered most of the substrate surface.

Figure 5 shows the SEM photographs of the Hf substrate after cathodic polarization and heat treatment, followed by soaking in SBF. After cathodic polarization, many pores with sizes of approximately 1 μm were observed. After the heat treatment, needlelike crystals were observed. After subsequent soaking in SBF, spherical particles covered the surface of the substrate. Figure 6 shows the TF-XRD pattern of the same samples. Hafnium hydride was formed after cathodic polarization, and it was completely converted to monoclinic HfO_2 after the heat treatment. Apatite peaks were detected after the samples were soaked in SBF.

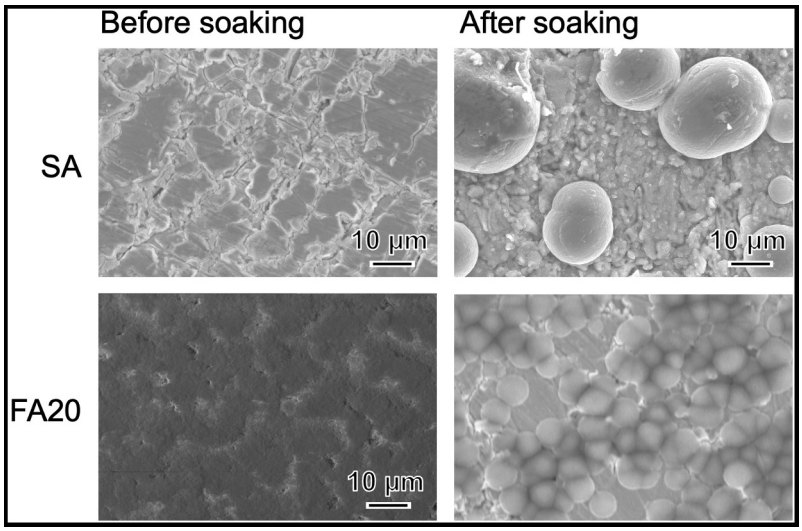

Figure 2. SEM photographs of SA and FA20 before and after soaking in SBF. Soaking time is 7 days for SA and 8 days for FA20.

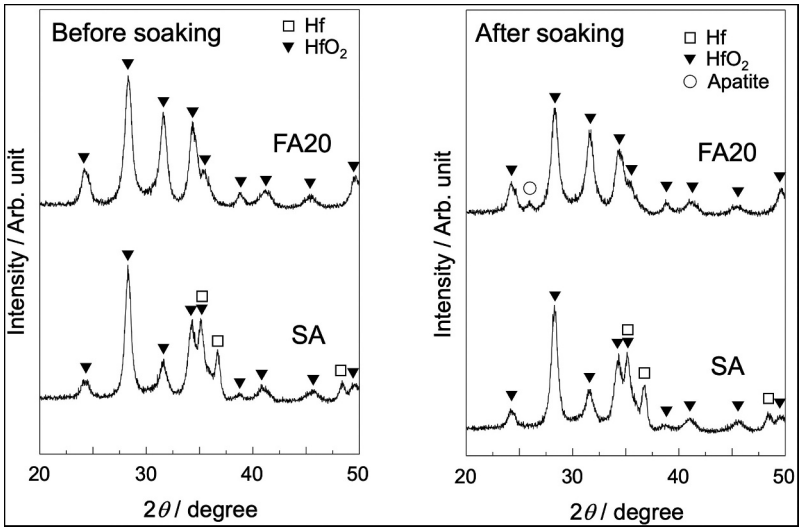

Figure 3. TF-XRD patterns of SA and FA20 before and after soaking in SBF. Soaking time is 7 days for SA and 8 days for FA20.

Table 2. Elemental composition of the apatite formed on FA20.

Element	Atomic ratio (%)
O	27.1
F	0.14
P	25.8
Ca	46.4
Hf	0.58

Figure 7 shows SEM photographs of the Hf substrate after it was soaked in NH_4F solution, heat-treated, and subsequently soaked in SBF. After NH_4F treatment, a porous morphology was observed, and the pores were 2 to 3 μm in size. This morphology did not change significantly after the heat treatment. After soaking in SBF, the substrate surface was covered with newly formed particles. Figure 8 shows the TF-XRD pattern of the same surfaces. Only Hf peaks (JCPDS #38-1478) were observed after NH_4F treatment, and monoclinic HfO_2 peaks were detected after the heat treatment. Apatite peaks were detected after soaking in SBF.

Table 3 shows the contact angles using ultrapure water and the surface energies of the samples. The contact angle increased in the order of FA20<SA<FS<FC, whereas the surface energy decreased in the order of FA20>SA>FS>FC.

4. Discussion

4.1. Surface morphology and chemical composition

The HfO_2 crystalline phase was observed on all the sample surfaces after heat treatment, although the morphology was different among the surfaces. That is, nanotubes were observed on the surface of FA20, whereas micropores were observed for FC and FS. In the case of FC, the hafnium hydride formed by cathodic polarization decomposed under heat treatment to form numerous pores. Titanium hydrides have been reported to play the role of pore-forming agents [20].

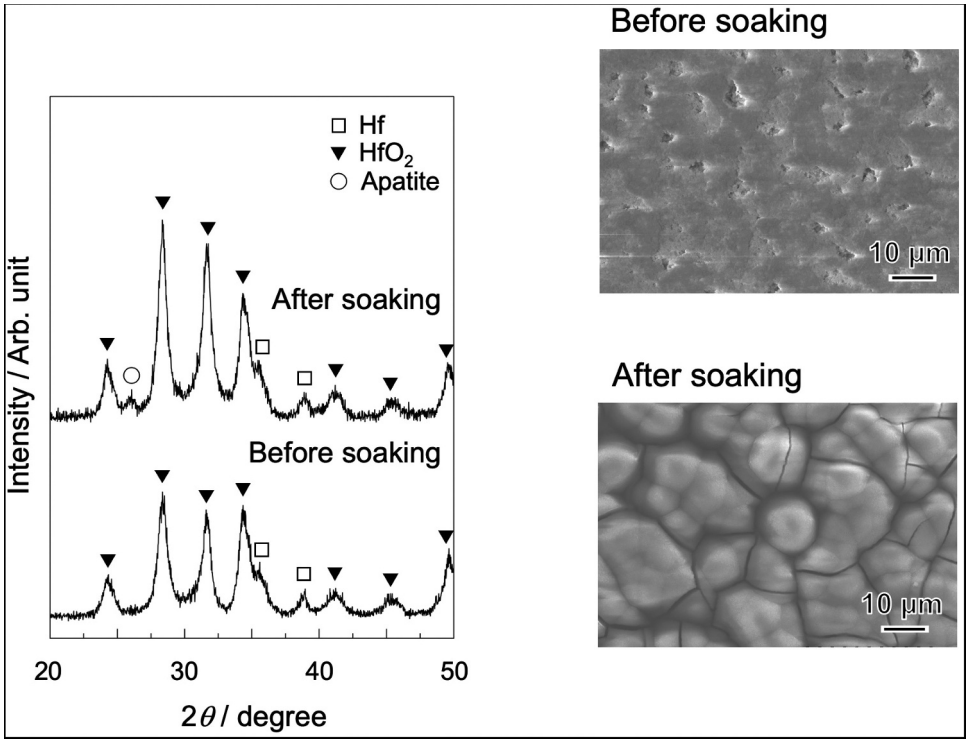

Figure 4. SEM photographs and TF-XRD patterns of FA60 before and after soaking in SBF for 3 days.

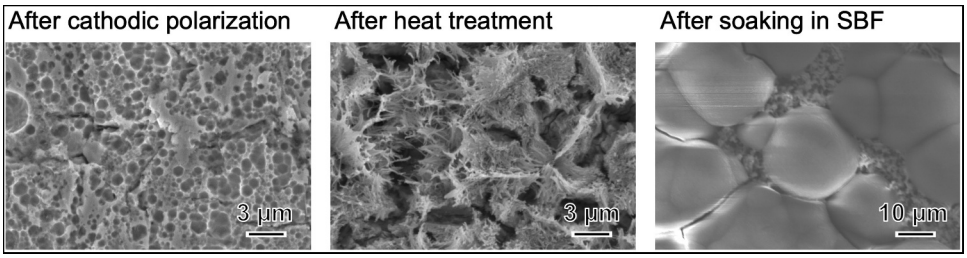

Figure 5. SEM photographs of Hf substrates after cathodic polarization in NH_4F solution and heat treatment, followed by soaking in SBF for 8 days.

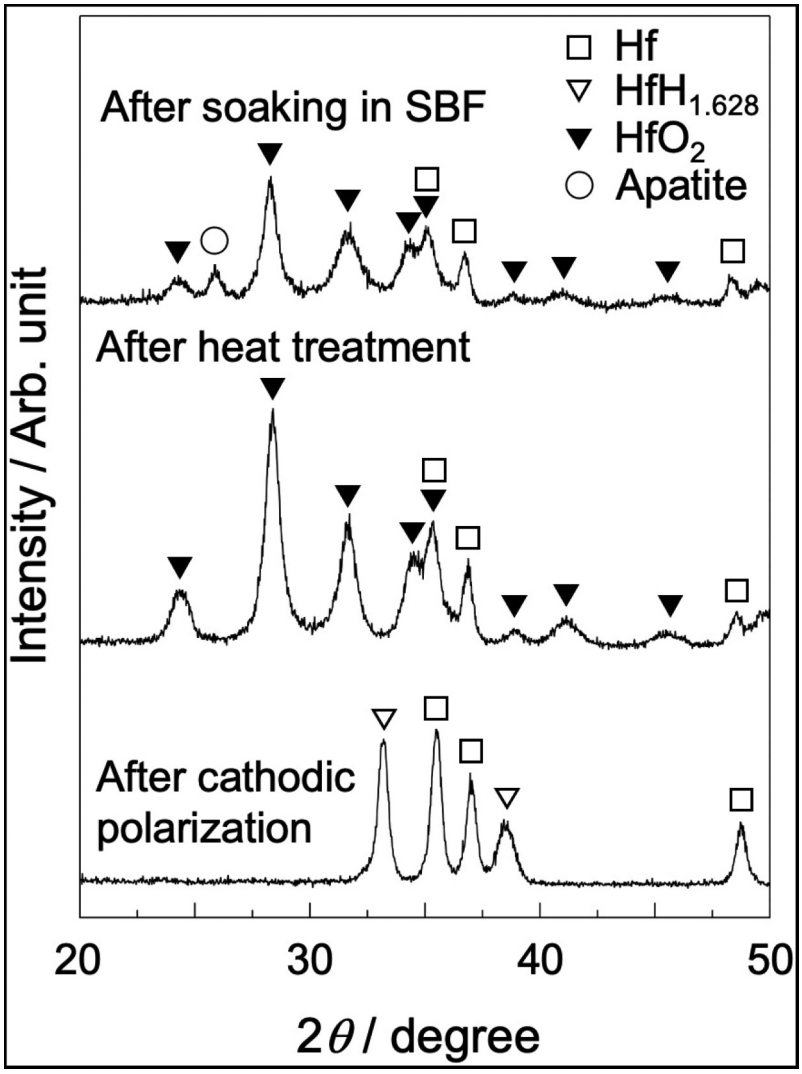

Figure 6. TF-XRD patterns of Hf substrates after cathodic polarization in NH_4F solution and heat treatment, followed by soaking in SBF for 8 days.

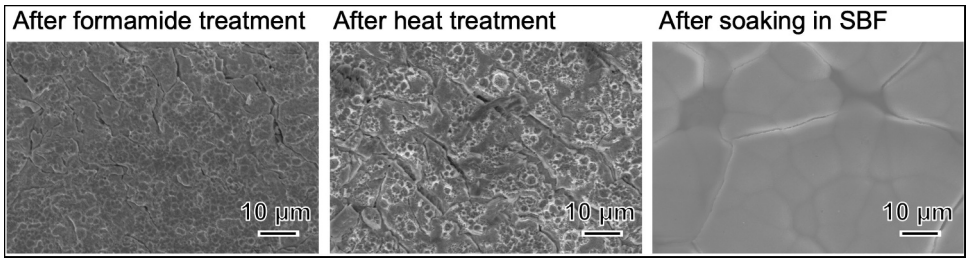

Figure 7. SEM photographs of Hf substrates after soaking in NH_4F solution and heat treatment, followed by soaking in SBF for 7 days.

Yang *et al*. reported that although few pores form on the surface of Ti anodically polarized at low voltages, the surface becomes highly porous when it encounters spark discharges at voltages greater than 150 V [15]. Because no spark discharge occurred during the preparation of SA, the present results are consistent with this report. In the present study, apatite formation was induced by electrochemical polarization at voltages lower than 50 V or by soaking in NH_4F solution. Therefore, the present methods are safe surface modification processes.

Among the samples treated with NH_4F solution, FS did not contain F on its surface. When Ti is anodically polarized in NaF solution, the formed TiO_2 reacts with NaF to give a fluoro titanium complex according to the following reactions [21]:

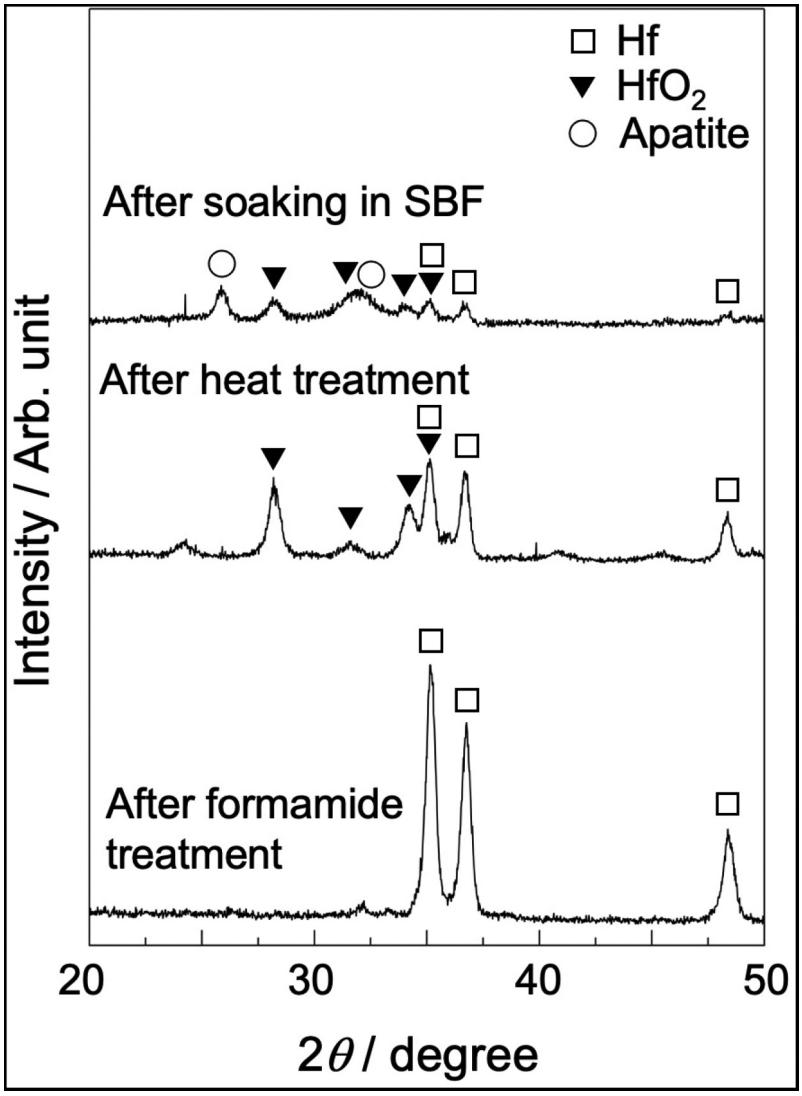

Figure 8. TF-XRD patterns of Hf substrates after soaking in NH_4F solution and heat treatment, followed by soaking in SBF for 7 days.

Table 3. Contact angle using ultrapure water and surface energy of the samples.

Sample	Contact angle/°	Surface energy γ_s/mJ·m^{-2}
SA	32.3 ± 0.4	67.7
FA20	4.93 ± 0.850	75.7
FC	76.3 ± 0.306	43.5
FS	58.9 ± 0.404	52.8

$$Ti + 2H_2O \rightarrow TiO_2 + 4H^+ + 4e^- \quad (3)$$

$$TiO_2 + 6F^- + 4H^+ \rightarrow [TiF_6]^{2-} + 2H_2O \quad (4)$$

Therefore, F was not incorporated into FS because a HfO_2 layer did not form on its surface by mere soaking in NH_4F (Figure 8).

Chen *et al*. investigated the surface structure of Ti soaked in NaF solution under various conditions [22]. When Ti was soaked in NaF aqueous solution at pH 7.3, the F content determined using X-ray photoelectron spectroscopy (XPS) was approximately 0.5%, and the F content increased with a decrease in pH. XPS generally detects chemical composition on a thin surface layer less than 10 nm in thickness. There is a possibility that a small amount of F was incorporated into FS. However, in the case of FC, F was incorporated into the surface because F^- is attracted to the cathode in the applied electric field.

4.2. Apatite-forming ability

In a previous study, although the spherical particles formed in SBF were observed in a part of the Hf substrate treated with NaOH and heat, they were not identified as apatite using TF-XRD [14]. However, apatite was detected using TF-XRD when Hf was treated in NH_4F solution (Figures 3,4,6,8). Therefore, the apatite-forming ability of Hf should be improved by the present method.

Although all the samples had a layer of HfO_2, the apatite-forming ability of each sample in SBF was different. Namely, the TF-XRD pattern of SA did not contain diffraction peaks arising from apatite. It is likely that the formed calcium phosphate is amorphous or its amount is small. However, the apatite-forming ability of the samples treated in the fluoride solution was

higher than that of SA. Among them, FS with the highest apatite/HfO_2 peak intensity ratio is considered to have an excellent apatite-forming ability.

The degree of apatite formation in SBF was similar between FA20 after 8 days and FA60 after 3 days, indicating that an increase in anodic polarization time in NH_4F solution up to 60 min increased the amount of formed HfO_2 nanotubes, which in turn increased the amount of apatite formed.

For both anodic and cathodic polarizations, if the internal resistance of the polarization apparatus is R, the amount of electricity required to prepare FC (Q_{FC}) can be calculated as follows:

$$Q_{FC} = It = \left(\frac{15}{R} + \frac{30}{R} + \frac{45}{R}\right) \times 20 \times 60 = \frac{108000}{R} \quad (5)$$

Assuming that the internal resistance is the same as in cathodic polarization, the amount of electricity required to prepare FA60 (Q_{FA60}) can be calculated as follows:

$$Q_{FA60} = It = \frac{30}{R} \times 60 \times 60 = \frac{108000}{R} \quad (6)$$

Therefore, both amounts of electricity are equal. HfO_2 formation by anodic polarization is described as follows:

$$Hf + 2H_2O \rightarrow HfO_2 + 4H^+ + 4e^- \quad (7)$$

However, hafnium hydride formation by cathodic polarization is described as follows:

$$Hf + 1.628H^+ + 1.628e^- \rightarrow HfH_{1.628} \quad (8)$$

For the same amount of electricity, the amount of hafnium hydride formed on the cathode is 2.5 times that of HfO_2 formed on the anode. Considering that the degree of apatite formation in SBF is almost equivalent between FA60 after 3 days and FC after 8 days, the apatite-forming ability of the anodically formed HfO_2 is superior to that of the cathodically formed hydride.

It has been reported that the higher the surface energy of surface-treated titanium, the greater the apatite-forming ability [23,24]. However, in this study, no correlation was found between surface energy and apatite-forming ability. For example, although SA had a relatively high surface energy, its apatite-forming ability was low. The surface energy shown in Table 3 is a value per unit area, and therefore the actual total surface energy differs depending on the surface topology [25]. Because there is no difference in the surface crystalline phase, the differences in apatite formation likely arise from differences in the pore structure. The above postulate is supported by previous results that the greater the roughness of the Ti, Zr, and Ti-Zr alloy treated with NaOH and heat, the higher the apatite-forming ability [26]. An increase in specific surface area also enhances the adsorption of Ca and P in SBF as a precursor of apatite.

When the Hf substrates were electrochemically polarized in NH_4F solution, F was incorporated into the surfaces of the substrates (Table 1). F was also detected in the formed apatite (Table 2). F is known to stabilize apatite crystals [27], although when bone-bonding bioactive glass contains an excessive amount of F (approximately 10%), CaF_2 is formed in SBF to suppress apatite formation [28]. In this study, even F-free FS showed excellent apatite formation, suggesting that F plays a minor role in enhancing apatite formation.

Aita *et al*. demonstrated that adding F to modified SBF produces highly oriented apatite crystals, similar to that of tooth enamel [29]. In future, morphological control of apatite may be possible by changing the F content of the electrolyte.

5. Conclusions

In summary, we investigated the apatite-forming ability of surface-modified Hf metal in SBF. Hf substrates were electrochemically polarized in H_2SO_4 or NH_4F solution or soaked in NH_4F solution and then heated at 600°C for 1 h. NH_4F treatment was more effective than H_2SO_4 treatment in imparting the metal with enhanced apatite-forming ability. Among the surface modification methods investigated, soaking the Hf metal in NH_4F solution was the most effective for enhancing apatite formation. Notably, the surface pore structure, rather than the surface energy and F content, played a dominant role in apatite formation. In future studies, the effect of incorporated F amount on the orientation of the apatite crystal will be investigated. Findings of this study would help to clarify the basic principles governing the bone-bonding ability of artificial materials.

Acknowledgments

We thank Edanz (https://jp.edanz.com/ac) for editing a draft of this manuscript.

Disclosure statement

No potential conflict of interest was reported by the author(s).

References

[1] Matsuno H, Yokoyama A, Watari F, et al. Biocompatibility and osteogenesis of refractory metal implants, titanium, hafnium, niobium, tantalum and rhenium. Biomaterials. 2001;22(11):1253–1262.

[2] Brånemark PI. Osseointegration and its experimental background. J Prosthet Dent. 1983;50(3):399–410.
[3] Yan WQ, Nakamura T, Kobayashi M, et al. Bonding of chemically treated titanium implants to bone. J Biomed Mater Res. 1997;37(2):267–275.
[4] Skripitz R, Aspenberg P. Tensile bond between bone and titanium: a reappraisal of osseointegration. Acta Orthop Scand. 1998;69(3):315–319.
[5] Hench LL. Bioceramics. J Am Ceram Soc. 1998;81 (7):1705–1728.
[6] Kokubo T, Kushitani H, Sakka S, et al. Solutions able to reproduce in vivo surface-structure changes in bioactive glass-ceramic A-W. J Biomed Mater Res. 1990;24 (6):721–734.
[7] Cho SB, Kokubo T, Nakanishi K, et al. Dependence of apatite formation on silica gel on its structure: effect of heat treatment. J Am Ceram Soc. 1995;78(7):1769–1774.
[8] International Organization for Standardization (ISO). Implants for surgery — in vitro evaluation for apatite-forming ability of implant materials. Geneve: ISO; 2014. Standard No. ISO 23317:2014.
[9] Kokubo T, Kim HM, Kawashita M, et al. Bioactive metals: preparation and properties. J Mater Sci Mater Med. 2004;15(2):99–107.
[10] Hanawa T. Titanium–tissue interface reaction and its control with surface treatment. Front Bioeng Biotech. 2019;7:170.
[11] Sato H, Kikuchi M, Komatsu M, et al. Mechanical properties of cast Ti–Hf alloys. J Biomed Mater Res B. 2005;72(2):362–367.
[12] Jeong YH, Choe HC, Brantley WA. Corrosion characteristics of anodized Ti-(10-40wt%)Hf alloys for metallic biomaterials use. J Mater Sci Mater Med. 2011;22(1):41–50.
[13] González M, Peña J, Manero J, et al. Design and characterization of new Ti-Nb-Hf alloys. J Mater Eng Perform. 2009;18(5–6):490–495.
[14] Miyazaki T, Sueoka M, Shirosaki Y, et al. Development of hafnium metal and titanium-hafnium alloys having apatite-forming ability by chemical surface modification. J Biomed Mater Res B: Appl Biomater. 2018;106B (7):2519–2523.
[15] Yang B, Uchida M, Kim HM, et al. Preparation of bioactive titanium metal via anodic oxidation treatment. Biomaterials. 2004;25(6):1003–1010.
[16] Zwilling V, Darque-Ceretti E, Boutry-Forveille A, et al. Structure and physicochemistry of anodic oxide films on titanium and TA6V alloy. Surf Interf Anal. 1999;27 (7):629–637.
[17] Miyabe S, Fujinaga Y, Tsuchiya H, et al. Fabrication of bottle-shaped TiO_2 nanotubes for drug delivery system. Poster session presented at: 30th Annual Conference of the European Society for Biomaterials; 2019Sep9-13; Dresden, Germany.
[18] Qiu X, Howe JY, Meyer HM, et al. Thermal stability of HfO_2 nanotube arrays. Appl Surf Sci. 2011;257 (9):4075–4081.
[19] Owens DK, Wendt RC. Estimation of the surface free energy of polymers. J Appl Polym Sci. 1969;13 (8):1741–1747.
[20] Li H, Yuan B, Gao Y, et al. High-porosity NiTi superelastic alloys fabricated by low-pressure sintering using titanium hydride as pore-forming agent. J Mater Sci. 2009;44(3):875–881.
[21] Yun JH, Ng YH, Ye C, et al. Sodium fluoride-assisted modulation of anodized TiO2 nanotube for dye-sensitized solar cells application. ACS Appl Mater Interfaces. 2011;3(5):1585–1593.
[22] Chen WQ, Zhang SM, Qiu J. Surface analysis and corrosion behavior of pure titanium under fluoride exposure. J Prosthet Dent. 2020;124(2):239.e1–239.e8.
[23] Wang X, L Y, Lin J, et al. Apatite-inducing ability of titanium oxide layer on titanium surface: the effect of surface energy. J Mater Res. 2008;23(6):1682–1688.
[24] Chen XB, Li YC, Hodgson PD, et al. The importance of particle size in porous titanium and nonporous counterparts for surface energy and its impact on apatite formation. Acta Biomater. 2009;5(6):2290–2302.
[25] Packham DE. Surface energy, surface topography & adhesion. Int J Adhes Adhes. 2003;23(6):437–448.
[26] Chen X, Nouri A, Li Y, et al. Effect of surface roughness of Ti, Zr, and TiZr on apatite precipitation from simulated body fluid. Biotechnol Bioeng. 2008;101(2):378–387.
[27] Okazaki M, Takahashi J, Kimura H, et al. Crystallinity, solubility, and dissolution rate behavior of fluoridated CO_3 apatites. J Biomed Mater Res. 1982;16(6):851–860.
[28] Brauer DS, Karpukhina N, O'Donnell MD, et al. Fluoride-containing bioactive glasses: effect of glass design and structure on degradation, pH and apatite formation in simulated body fluid. Acta Biomater. 2010;6(8):3275–3282.
[29] Aita K, Oaki Y, Ohtsuki C, et al. Fabrication of self-standing films consisting of enamel-like oriented nanorods using artificial peptide. CrystEngComm. 2015;17(29):5551–5555.